Journal of Catalysis **204,** 11–22 (2001)
doi:10.1006/jcat.2001.3359, available online at http://www.idealibrary.com on IDEAL®

The Formation and Hydrolysis of Isocyanic Acid during the Reaction of NO, CO, and H_2 Mixtures on Supported Platinum, Palladium, and Rhodium

Dean C. Chambers, Dennys E. Angove,[1] and Noel W. Cant[2]

Department of Chemistry, Macquarie University, Sydney, New South Wales 2109, Australia

Received December 6, 2000; revised July 20, 2001; accepted July 20, 2001

The extent to which isocyanic acid (HNCO) is formed during the reaction of NO/CO/H_2 mixtures over silica-supported Pt, Rh, and Pd has been investigated together with the subsequent hydrolysis of HNCO on oxide systems placed downstream. The yield of HNCO from NO is highest for Pt/SiO_2 exceeding 35% at 315°C with a standard 2800/3400/1200 ppm NO/CO/H_2 mixture. Hydrogen consumption is complete at 220°C with ammonia and water as major products, but above 260°C HNCO becomes the favoured product with some arising from NH_3. Hydrolysis of HNCO to NH_3 and CO_2 takes over once all NO has been consumed. The extent of hydrolysis is increased somewhat if additional SiO_2 is placed downstream. Other oxide systems—CeO_2/SiO_2, BaO/SiO_2, CeO_2/Al_2O_3, and CeO_2-ZrO_2—give complete hydrolysis to the extent of the available water at 315°C, and no HNCO remains if additional water is included in the feed. Hydrogen consumption during the NO + CO + H_2 reaction commences at the lowest temperature on the Pd/SiO_2, and for 100°C from the onset temperature of 130°C the reaction can be largely described as the sum of the NO + H_2 and NO + CO ones. Formation of HNCO commences at 235°C, with a maximum yield of 20% at 300°C. It appears to arise solely through utilisation of NH_3 made as a side-product to the NO + H_2 reaction. Rh/SiO_2 is much less active than Pt/SiO_2 and Pd/SiO_2 for the NO + H_2 reaction, but more active for the NO + CO and NO + CO + H_2 ones. The latter exhibits a small sharp peak in HNCO formation, but the maximum yield is only 14% and this coincides with total consumption of NO. Considerable ammonia is formed at higher temperatures, even though none is produced during the NO + H_2 reaction. HNCO is believed to arise on each metal through the combination of surface hydrogen atoms with metal-bound NCO groups which exist in small numbers when N atoms are located adjacent to adsorbed CO molecules. The differences in behaviour between the metals can be rationalised in terms of the relative strengths of adsorption of CO and NO, and the temperature difference between total consumption of H_2 and NO. If the difference is large, then HNCO can be produced from ammonia as well as hydrogen. A general conclusion is that, although some HNCO might be generated on platinum group metal particles within the pores of three-way vehicle catalysts during warm-up, the rapidity of hydrolysis on oxide washcoats with water in large excess is so great that no HNCO would ever emerge. Only the hydrolysis products, NH_3 and CO_2, will be seen.

Key Words: **isocyanic acid; HNCO; Pt/SiO_2; Rh/SiO_2; Pd/SiO_2; hydrolysis; CeO_2; BaO; CeO_2–ZrO_2.**

INTRODUCTION

The reduction of NO by CO is the key reaction in conventional three-way catalysts used for emission control on motor vehicles (1). The reaction has been extensively studied, especially over rhodium, the most active platinum group metal (PGM). The most recent surface science studies using rhodium single crystals demonstrate that N_2O and N_2 are initially formed in parallel (2–5) by the reactions

$$2NO + CO \rightarrow N_2O + CO_2 \quad [1]$$

$$2NO + 2CO \rightarrow N_2 + 2CO_2, \quad [2]$$

although there have been claims that N_2O and N_2 are produced sequentially on supported rhodium (6, 7). The generally accepted mechanism with Rh, Pt, and Pd is that NO dissociates to form adsorbed N and O adatoms, the latter reacting with CO to form CO_2 while the former either dimerise to N_2 or react with adsorbed NO to yield N_2O (8). For supported PGMs the reaction is accompanied by the accumulation of isocyanate species (9–11), now known to be largely on the support (12, 13). Metal-bound isocyanates are also well established (14–17) and have been included in some reaction schemes (18), but the general belief is that they are too unstable to play a major role during steady-state catalysis.

Real exhaust contains other reducing agents, notably H_2 at approximately one-third the concentration of CO as set by the water–gas shift equilibrium at high temperature. Despite the importance of reductant mixtures, there have been few detailed studies of such systems for supported metals since the original comparative work of Kobylinski and Taylor (19) using percent level concentrations. They

[1] Present address: CSIRO Division of Energy Technology, P.O. Box 136, North Ryde, NSW 1670, Australia.

[2] To whom correspondence should be addressed. Fax: 61-2-9850-8313. E-mail: noel.cant@mq.edu.au.

0021-9517/01 $35.00

showed that the $NO + H_2$ reaction is faster than the NO+CO one on alumina-supported Pt, Pd, and Rh, the difference in activity being least for Rh. Activity for the $NO + CO + H_2$ reaction is intermediate between the individual ones but closer to that of the NO + CO one due to CO inhibition of hydrogen adsorption. Ammonia is formed as an undesired product, especially with platinum and palladium (20), which is partly responsible for the unsatisfactory performance of Pt alone as a three-way catalyst.

Discussion of the reaction of $NO/CO/H_2$ mixtures over supported PGMs in emission control catalysts has generally been on the basis that the $NO + H_2$ and NO + CO reactions proceed competitively with the individual characteristics observed for binary mixtures. However, work by Voorhoeve and Trimble (21) more than two decades ago showed that the reaction of a CO-rich ternary mixture over unsupported PGMs gives high yields of isocyanate compounds in trapped products, predominantly ammonium cyanate (NH_4NCO) with Pt and Rh but isocyanic acid (HNCO) with Pd and Ir (21–25).

More recently we have demonstrated, through online analysis using FTIR, that HNCO is a major gaseous product when NO, CO, and H_2 are reacted together over Pt/SiO_2 (26–28). The mechanism inferred was that a small number of Pt-bound NCO groups existed in equilibrium with N adatoms and adsorbed CO, and that these Pt–NCO groups gave rise to HNCO by reaction with H adatoms. No HNCO was seen when Al_2O_3 was placed downstream of Pt/SiO_2 or with a Pt/Al_2O_3 catalyst. Nonetheless, combined *in situ* FTIR/isotope studies using Pt/Al_2O_3 showed that support-bound NCO groups were present and that approximately 60% of all CO_2 formed passed through these NCO species when the feed contained some water (29). The conclusion was that HNCO was a significant short-lived gas-phase intermediate, desorbing from Pt and then undergoing facile hydrolysis to CO_2 and NH_3 after adsorption on alumina. Tests with more complex simulated exhaust mixtures over Pt/Al_2O_3 and $Pt/CeO_2/Al_2O_3$ also indicate that the ammonia formed in such systems during light-off under near stoichiometric conditions is derived by that route (30).

The purpose of the present work was twofold. First, we sought to establish if isocyanic acid is formed during the $NO + CO + H_2$ reaction over silica-supported Pd and Rh in the same way as with Pt/SiO_2, given that the alumina-supported metals differ considerably in their tendency to make ammonia (19). The only previous study here is that of Hecker and Bell (31) for Rh/SiO_2 who observed the formation of solid urea, an isomer of ammonium isocyanate, with a reduced catalyst and suspected, but were unable to prove, the formation of HNCO when the catalyst was pre-oxidised. Our second purpose was to determine if isocyanic acid undergoes hydrolysis to CO_2 and NH_3 as easily and completely on other oxides as it does on alumina. This is of some importance since CeO_2–ZrO_2 is now the preferred washcoat for three-way catalysts, and other oxides, such as BaO, are of interest as the basis for the nitrate storage catalysts developed for use with intermittent lean burn engines (32).

EXPERIMENTAL

The catalytic reactions were carried out as outlined previously (28). Samples of catalyst (weighing 75 mg), and downstream oxides (also 75 mg if present), were held between quartz wool plugs in a 4-mm i.d. Pyrex tube in a tube furnace. The test mixtures were made up by blending analysed mixtures (BOC Aust.) using electronic mass flow controllers (Brooks 5850TR). The outlet stream was periodically sampled by a micro gas chromatograph (MTI Instruments model M200), for analysis of H_2 and N_2, and then flowed through heated 1/16-in. o.d. stainless-steel tubing to a 16-cm pathlength infrared cell in a box maintained at 90°C. The concentrations of CO, CO_2, NO, N_2O, NH_3, and H_2O were obtained using the software program MALT (33) to process spectra, recorded as 64 scans at 0.25-cm^{-1} resolution on a Nicolet Magna 550 FTIR with an MCT detector, against a set of synthetic spectra constructed from the HITRAN database (34). This procedure is in principle an absolute method if absorbances of the target compounds are within appropriate bounds, as was confirmed by flowing single and multicomponent mixtures of known concentration. The concentration of HNCO was calculated from the absorbance of its band at 2284 cm^{-1} as described previously (28), but with a slightly revised calibration factor (ppm = 3470 × absorbance at 2284 cm^{-1} after correction for CO_2). The analyses for carbon and nitrogen-containing compounds are believed accurate to better than 10% since the corresponding mass balances were seldom outside this limit. Hydrogen and water analyses are somewhat less accurate due to the low sensitivity of the gas chromatograph detector for H_2 and hold-up of water on the catalyst and system walls.

The Pt/SiO_2 and Pd/SiO_2 catalysts were from the series prepared and characterised in detail by Uchijima *et al.* (35) and Pitchai *et al.* (36). The Pt/SiO_2 (1.1 wt% Pt, 40% dispersion, designated 40–SiO_2–PtCl–L in Ref. (35)) was prepared by impregnation of silica gel (Davison grade 62, 285 m^2/g) with chloroplatinic acid and Pd/SiO_2 (0.49 wt% Pd, 79% dispersion, batch 79.1-Pd/SiO_2–IV in Ref. (36)) by ion exchange with $Pd(NH_3)_4(NO_3)_2$. The Rh/SiO_2 used the same base silica and was made here by impregnation to incipient wetness with a solution of $RhCl_3$ to a metal content of 0.50%, dried overnight at 140°C, and reduced in 10% H_2/He on a 1°C/min ramp ending with 2 h at 350°C. The dispersion, as determined by H_2 chemisorption in a flow system, was 38% which agreed with estimates from transmission electron microscopy showing rounded metal particles of diameter ∼3 nm. Thus the number of surface

metal atoms in the three catalysts on a weight of catalyst basis is in the approximate ratio Pd : Pt : Rh = 2.0 : 1.2 : 1.0.

The 10 wt% BaO/SiO_2 sample was made as for Rh/SiO_2 with impregnation of a nitrate solution followed by drying and calcination in air at 640°C with exposure to 2000 ppm CO_2/He for 40 min at 400°C during cooling to minimise carbon dioxide uptake in subsequent tests. The CeO_2/Al_2O_3 (22 wt%CeO_2, surface area 140 m^2/g) and CeO_2–ZrO_2 (Ce : Zr mol ratio 1 : 1, 143 m^2/g) samples were commercial materials used in the manufacture of three-way catalytic converters and provided by Johnson–Matthey Catalytic Systems Division.

Testing of each sample of catalyst was commenced by ramping the temperature up and down in the standard NO + CO mixture (~2900 and ~3400 ppm, respectively) until behaviour was stable. The NO + CO, NO + H_2 (~2000 and ~1100 ppm, respectively), and NO + CO + H_2 (~2900, ~3400, and ~1100 ppm, respectively) reactions were then carried out in turn by ramping the catalyst at 2°C/min with analyses every 10 min. Mass balance calculations indicated that the ramp rate was sufficiently slow to avoid transient adsorption effects for all substances present except water.

RESULTS

Reactions on Pt/SiO_2

The two individual reactions were investigated first. As illustrated by Fig. 1A, the NO + H_2 reaction occurs at a much lower temperature than the NO + CO one on Pt/SiO_2 with complete H_2 consumption by 80°C. At low temperature the dominant product is N_2O,

$$2NO + H_2 \rightarrow N_2O + H_2O, \qquad [3]$$

which matches the NO/H_2 ratio of two in the feed. After H_2 consumption is complete, formation of NH_3 increases with temperature so that it becomes the major product between 150 and 200°C. At higher temperatures still, formation of NH_3 declines to zero, and N_2 and N_2O grow with the former taking over as the major product, especially so above 350°C. It should be noted here that the product distribution is highly dependent on the input NO/H_2 ratio. With 2000 ppm NO and 5000 ppm H_2 (not shown), NH_3 was the dominant product at all temperatures above 100°C in accord with the literature (37, 38).

The NO + CO reaction (Fig. 1B) commences at ~250°C on Pt/SiO_2 with complete conversion of NO by 380°C. Nitrous oxide is the dominant nitrogen-containing product at intervening temperatures with peak production of 1220 ppm at 330°C and a N_2O selectivity ($N_2O/(N_2O+N_2)$) of 82%. Nitrogen takes over as the major product above 360°C and becomes the sole one above 390°C.

Figure 2 shows the exit gas concentrations during the reaction of NO + CO + H_2 reaction over Pt/SiO_2 with

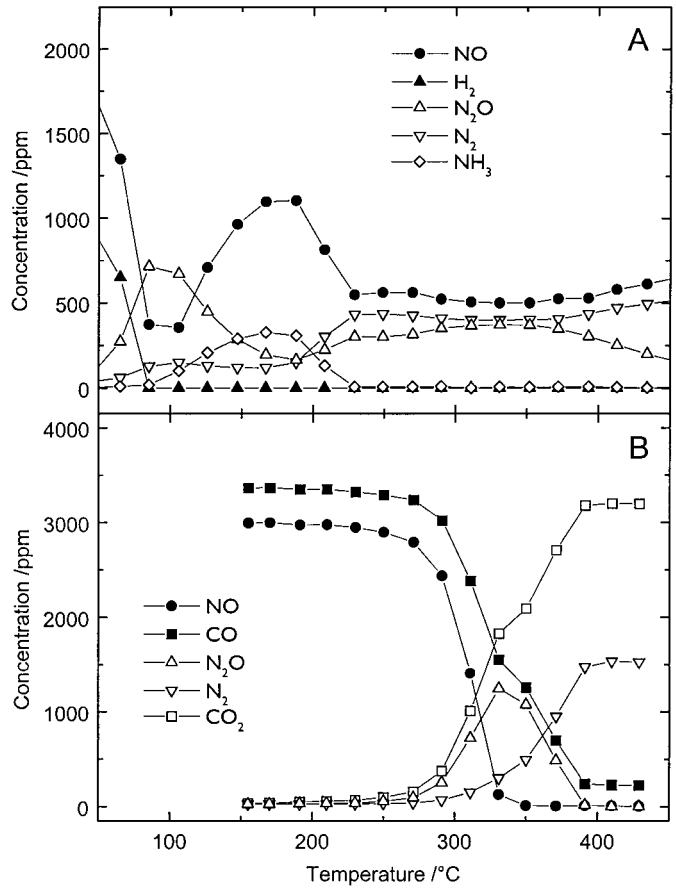

FIG. 1. Concentrations versus temperature for binary reactions over 75 mg Pt/SiO_2. (A) 1900 ppm of NO with 1100 ppm H_2. (B) 3000 ppm NO with 3400 ppm CO and a total flowrate of 100 cm^3/min.

reactant concentrations and CO_2 shown in Fig. 2A and all products, including CO_2, on an expanded scale in Fig. 2B. Carbon monoxide greatly inhibits the reaction of hydrogen in the NO + CO + H_2 system with an onset temperature of ~150°C for formation of N_2O and H_2O, compared with near room temperature for the NO + H_2 reaction on its own (Fig. 1A). The amount of CO_2 made throughout the consumption of NO and H_2 is several times greater than observed for the NO + CO reaction. Thus the presence of H_2 promotes CO consumption as noted previously (39). Formation of ammonia approximates that of CO_2 while H_2 is being consumed, but then passes through a maximum. Isocyanic acid is measurable from the onset of reaction with a shoulder in its concentration near 250°C. This is followed by a steep rise to a maximum of 1020 ppm at 316°C (a yield relative to the input NO of ~36%) that coincides with a minimum in NH_3 concentration. At higher temperatures HNCO production declines in concert with a fall in H_2O concentration, and a rise in NH_3 and CO_2 formation, as expected for hydrolysis:

$$HNCO + H_2O \rightarrow NH_3 + CO_2. \qquad [4]$$

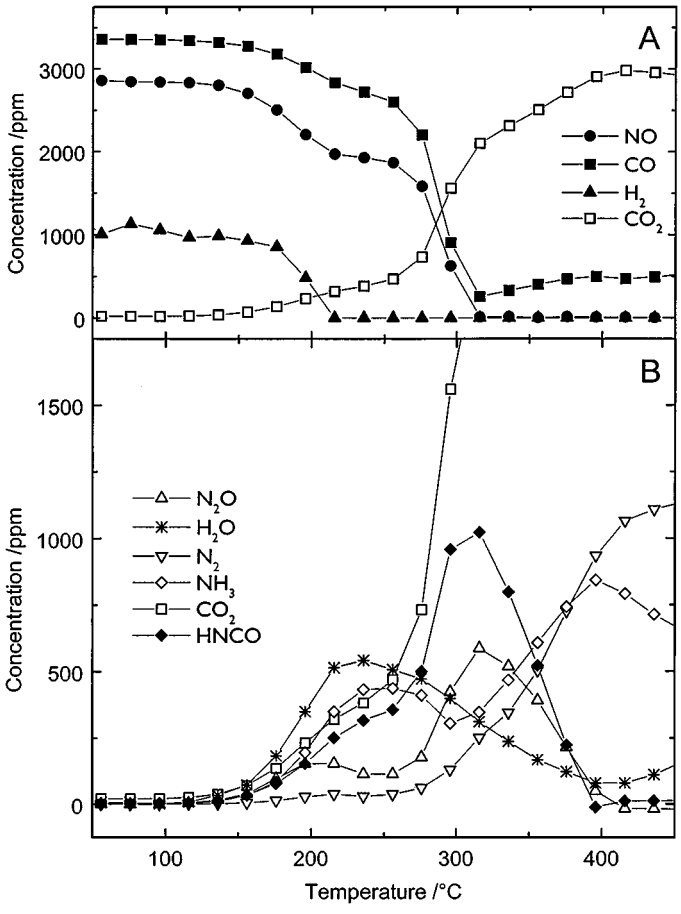

FIG. 2. Concentrations versus temperature for the reaction of 2800 ppm NO, 3400 ppm CO, and 1200 ppm H_2 over 75 mg Pt/SiO_2 with a total flowrate of 100 cm^3/min. (A) Reactants plus CO_2. (B) All products.

The general pattern for the $NO + CO + H_2$ reaction is similar to that seen previously with a reactant mixture with approximately two-thirds the concentrations (26, 27), but the HNCO concentrations are considerably higher. More accurate analyses, better overall with hydrogen and water for the first time, also allow a more detailed definition of the key processes as explained later.

Reactions on Pd/SiO_2

Figures 3 and 4 show the corresponding results for the three reactions over Pd/SiO_2. Its activity for the $NO + H_2$ reaction (Fig. 3A) is slightly less than that of Pt/SiO_2. Again, N_2O formation by reaction [3] dominates initially with nitrogen taking over above 200°C. Formation of ammonia is less than with Pt/SiO_2 but, as in that system, it increased greatly in experiments with H_2 in 2.5-fold excess (not shown). The activity of Pd/SiO_2 for the NO + CO reaction (Fig. 3B) is greater than that of Pt/SiO_2 with a somewhat different temperature profile. Formation of N_2O peaks at a lower concentration (960 ppm, selectivity ~62%) but is spread out over a wider range of temperature. A distinct shoulder in CO removal, followed by a rise in N_2 production, indicates the presence of a slower second-stage reaction between N_2O and CO.

The behaviour of the ternary mixture over Pd/SiO_2 is shown in Fig. 4. Hydrogen consumption requires a higher temperature than for the corresponding $NO + H_2$ reaction, but the elevation in temperature is much less than for Pt/SiO_2 so inhibition by CO is less. As with the $NO + H_2$ reaction alone, nitrous oxide is formed initially with N_2 and NH_3 increasing once H_2 consumption is complete. Formation of CO_2 is similar to that for the NO + CO reaction on its own. HNCO is not evident until 235°C, 75°C above the temperature at which H_2 consumption is complete, and exhibits a peak of ~550 ppm near 300°C (a yield of 20%). Thus the combined system appears to comprise a rapid $NO + H_2$ reaction, which will be increasingly confined to the front of the bed as temperature rises, a slower parallel NO + CO reaction, and an even slower process generating HNCO above 230°C.

The standard concentrations used above were chosen in part to maximise the formation of HNCO with Pt/SiO_2

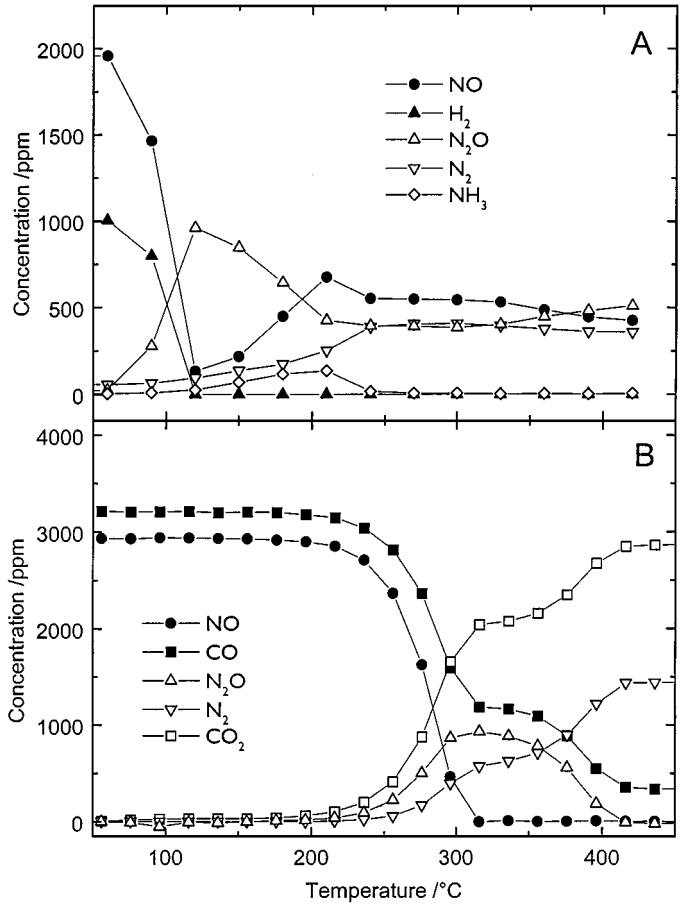

FIG. 3. Concentrations versus temperature for the binary reactions over 75 mg Pd/SiO_2. (A) 2000 ppm NO with 1000 ppm H_2. (B) 2900 ppm NO with 3450 ppm CO and a total flowrate of 100 cm^3/min.

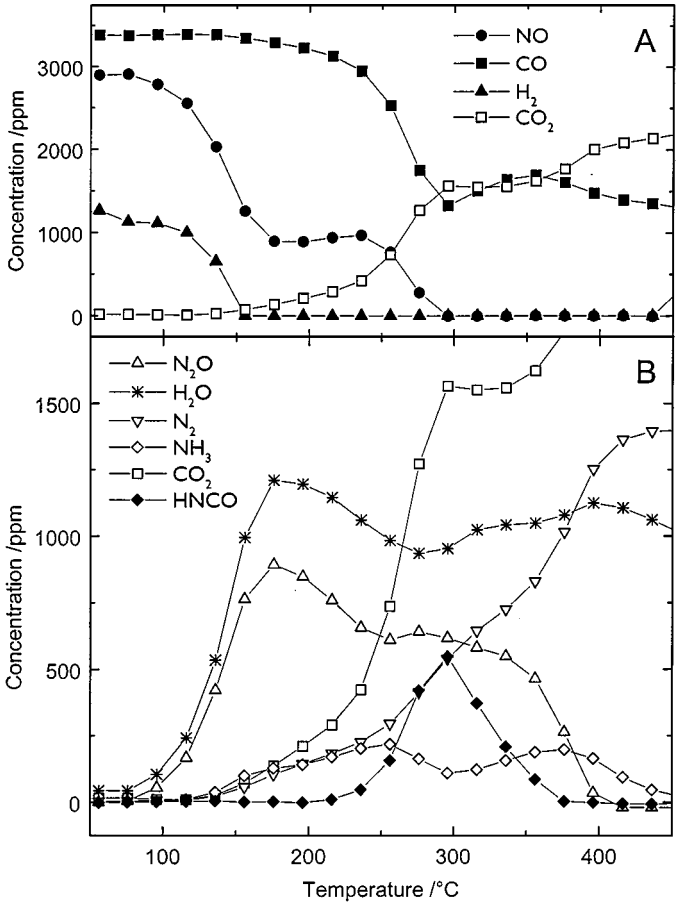

FIG. 4. Concentrations versus temperature for the reaction of 2900 ppm NO, 3400 ppm CO, and 1200 ppm H_2 over 75 mg Pd/SiO_2 with a total flowrate of 100 cm^3/min. (A) Reactants plus CO_2. (B) All products.

based on previous measurements of the pressure dependencies in that system (29). However, such concentrations are not necessarily optimal for the production of HNCO with the other PGMs. The pressure dependencies of HNCO production over Pd/SiO_2 at 282°C, when the NO conversion is ~80% with the standard feed, are plotted in Fig. 5. HNCO formation is favoured by higher H_2 and CO concentrations, as with Pt/SiO_2 (29), and exhibits a maximum for NO concentrations somewhat below the standard one.

Reactions on Rh/SiO_2

Data for the individual reactions over Rh/SiO_2 are shown in Fig. 6. The $NO + H_2$ reaction (Fig. 6A) is much slower than for Pt/SiO_2 or Pd/SiO_2 and produces N_2O and N_2 in the approximate ratio of 4 : 1 during H_2 consumption. Ammonia is not a product under these conditions with NO in excess but, as with the other two PGMs, considerable amounts were formed when using a mixture with H_2 in substantial excess (not shown). The onset temperature for the NO + CO reaction (Fig. 6B) is similar to that for the $NO + H_2$ one and much lower than that required for Pt/SiO_2 and Pd/SiO_2. The

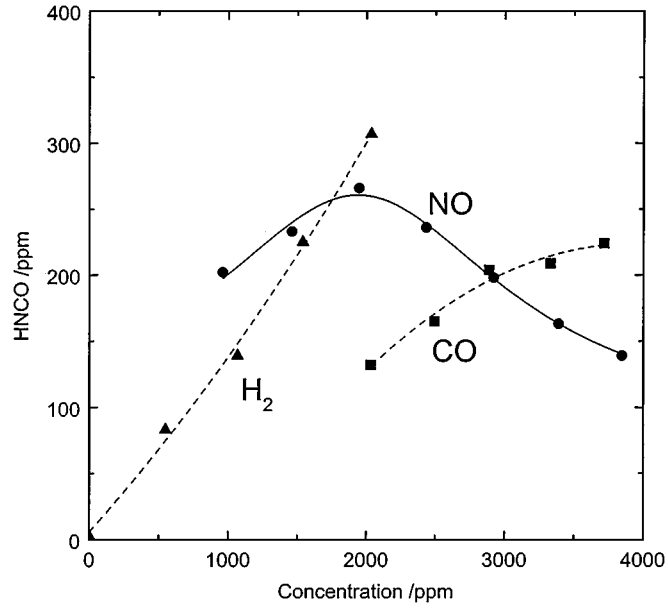

FIG. 5. Dependence of HNCO formation on individual concentrations over 75 mg of Pd/SiO_2 at 225°C when remaining concentrations are fixed (NO at 2900 ppm, CO at 3400 ppm, and H_2 at 1200 ppm).

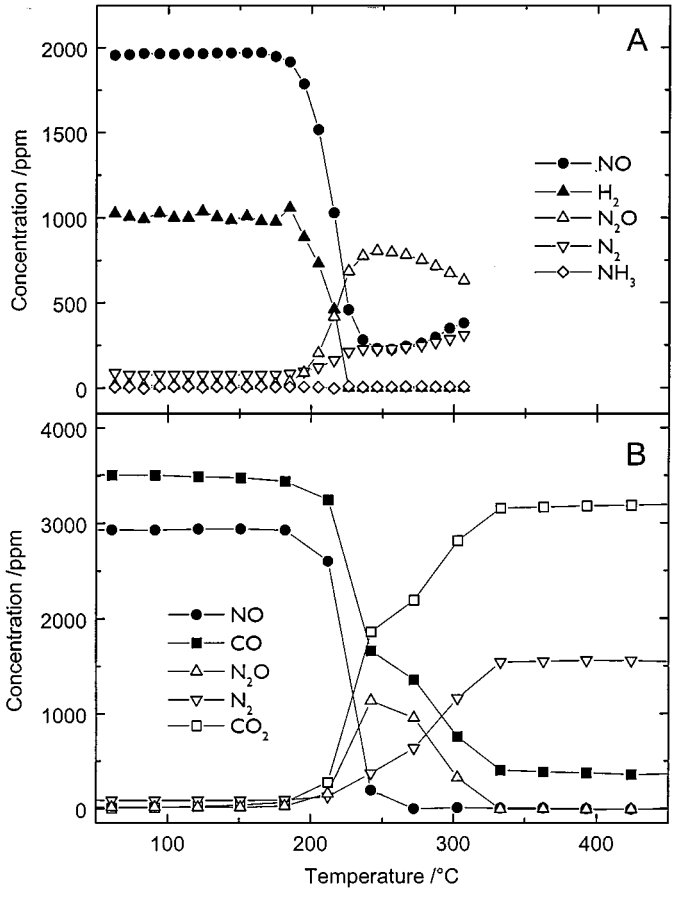

FIG. 6. Concentrations versus temperature for the binary reactions over 75 mg Rh/SiO_2. (A) 1950 ppm NO with 1000 ppm H_2. (B) 2900 ppm NO with 3500 ppm CO and a total flowrate of 100 cm^3/min.

reaction profile for Rh/SiO_2 is almost identical to that for Pt/SiO_2, but displaced to lower temperature by ~90°C. The maximum concentration of N_2O is ~1120 ppm at 240°C with a selectivity of 79%, very similar to that for the $NO + H_2$ reaction. Nitrogen formation takes over above 280°C with complete disappearance of N_2O by 330°C.

When NO, CO, and H_2 are reacted together over Rh/SiO_2 (Fig. 7), all three reactants are removed simultaneously over a narrow temperature interval (180 to 220°C). Production of HNCO shows a sharp peak at ~226°C, but the maximum concentration (400 ppm, 14% yield), and the temperature range over which it is seen, is much less than for Pt/SiO_2 or Pd/SiO_2. Unlike the $NO + H_2$ reaction over Rh/SiO_2, the ternary reaction yields considerable NH_3 which accounts for ~25% of the NO reacted between 250 and 300°C. Formation of N_2O passes through a maximum in a similar way to that for the NO + CO reaction. A minor feature of the ternary reaction over Rh/SiO_2 alone is the reformation of some hydrogen above 360°C, presumably by the water–gas shift reaction between residual CO and product water.

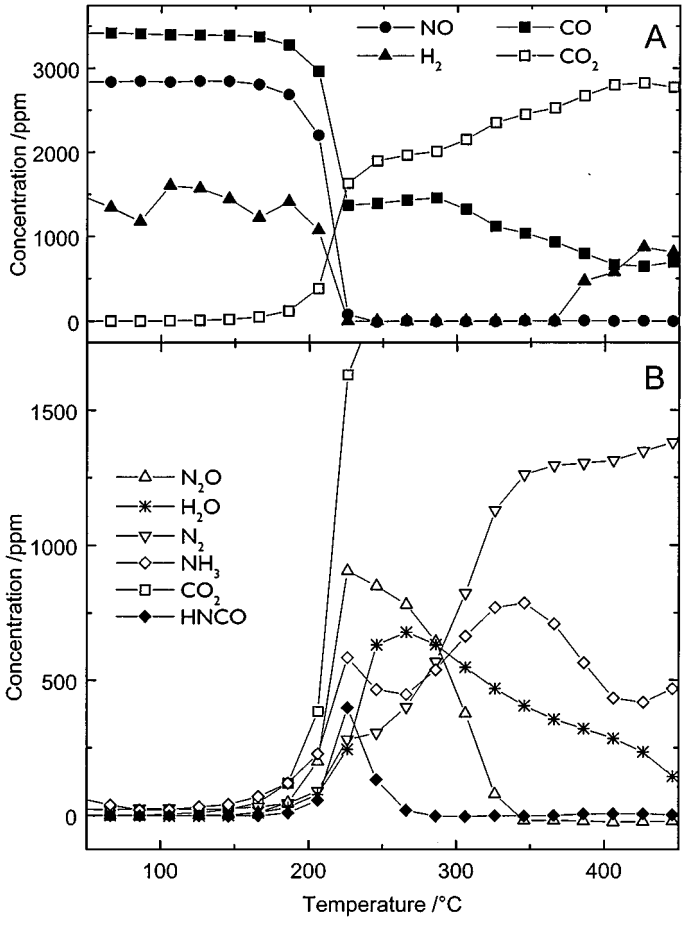

FIG. 7. Concentrations versus temperature for the reaction of 2800 ppm NO, 3450 ppm CO, and 1500 ppm H_2 over 75 mg Rh/SiO_2 with a total flowrate of 100 cm^3/min. (A) Reactants plus CO_2. (B) All products.

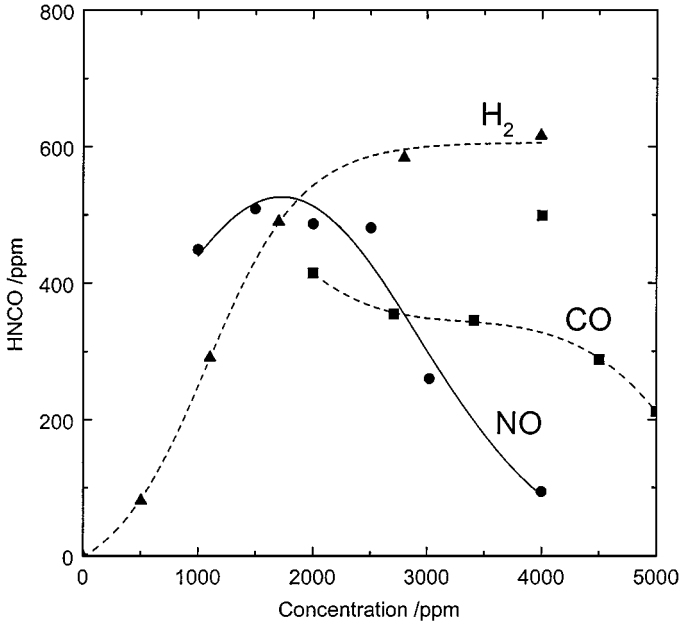

FIG. 8. Dependence of HNCO formation on individual concentrations over 75 mg of Rh/SiO_2 at 225°C when remaining concentrations are fixed (NO at 2900 ppm, CO at 3200 ppm, and H_2 at 1200 ppm).

Figure 8 shows how the HNCO concentration changed when the concentration of each reactant was varied in turn while the other concentrations were held constant at a temperature (225°C), giving ~60% NO conversion under standard conditions. Production of HNCO is increased if the concentrations of NO and CO are reduced relative to the standard ones or if higher H_2 concentrations are used. However, this result is likely to be dependent on the temperature as well, and no attempts have been made to maximise HNCO concentrations due to the extensive experimentation needed for optimisation in a four-dimensional system.

Hydrolysis of HNCO on Oxides

Our previous work on the further hydrolysis of HNCO on alumina placed downstream of Pt/SiO_2 was carried out at 230°C (27). As may be seen from Fig. 2, this temperature falls within a range in which production of water exceeds that of HNCO over Pt/SiO_2. Thus complete hydrolysis of HNCO according to Eq. [4] is feasible as was observed in practice both with Al_2O_3 downstream of Pt/SiO_2 and, separately, with a Pt/Al_2O_3 catalyst. However, data in Fig. 2 also show that the H_2O/HNCO ratio is less than unity at temperatures above 275°C. The hydrolysis/adsorption activity of other oxides has now been investigated in this regime. Figure 9 compares HNCO, H_2, and NH_3 concentrations during the $NO + CO + H_2$ reaction in two-random-order experiments, one using Pt/SiO_2 alone, the other a sequential bed of Pt/SiO_2 followed by CeO_2–ZrO_2. The presence of

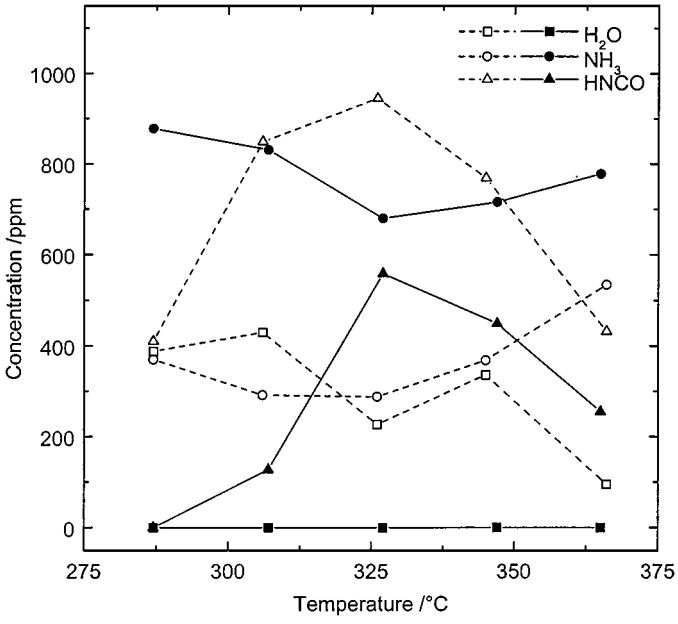

FIG. 9. Comparison of HNCO, NH_3, and H_2O concentrations during the NO + CO + H_2 reaction in one- and two-bed systems: open symbols, 75 mg of Pt/SiO_2 alone; closed symbols, 75 mg of Pt/SiO_2 followed by 75 mg of CeO_2–ZrO_2. Reactant concentrations and flowrates are the same as for Fig. 2.

CeO_2–ZrO_2 reduces the concentration of HNCO and H_2O with corresponding increases in formation of NH_3 (and also of CO_2, not shown). Indeed, since the H_2O concentration is zero with CeO_2–ZrO_2 present, reaction [4] has proceeded to the fullest extent possible at all temperatures. Also, since the reduction in HNCO concentration is largely balanced by the formation of the corresponding amount of additional NH_3, and CO_2, one can conclude that loss of HNCO by other processes, such as adsorption on the downstream oxide, is small.

On the basis of Fig. 9, one would expect more hydrolysis if additional water was available. Figures 10A and 10B compare the effect of adding ~1200 ppm water at 315°C when using Pt/SiO_2 alone with that using Pt/SiO_2, followed by an equal mass of SiO_2. With both systems the introduction of water is followed by stepwise loss of HNCO, ~25% for Pt/SiO_2 alone but ~50% for Pt/SiO_2 + SiO_2, with corresponding rises in the formation of NH_3 (and of CO_2, not shown). Thus SiO_2 alone has significant activity for HNCO hydrolysis. This explains the lower concentration of HNCO seen with the two-bed system compared to the single-bed one prior to the addition of water.

The results of similar experiments using sequential beds with BaO/SiO_2 and CeO_2/Al_2O_3 placed downstream of Pt/SiO_2 are shown in Fig. 11. Prior to water addition, the product stream with BaO/SiO_2 is completely dry. Correspondingly, the concentration of HNCO is lower, and that of NH_3 is higher, than with the Pt/SiO_2 and Pt/SiO_2 + SiO_2 systems (Fig. 10). Thus BaO/SiO_2 is able to hydrolyse HNCO to the limit of the water produced by the NO + CO + H_2 reaction. When additional water is introduced HNCO disappears altogether. The general behaviour of the Pt/SiO_2 + CeO_2/Al_2O_3 system is similar except that there is an initial delay in the formation of HNCO, with elevated NH_3 formation, that is attributable to HNCO hydrolysis on residual hydroxyl groups. The steady-state concentration of HNCO also appears slightly lower than that with BaO/SiO_2, which may reflect some accumulation of surface isocyanate groups. This would explain why the complete hydrolysis of HNCO that occurs on subsequent introduction of water gives rise to a higher concentration of ammonia than with BaO/SiO_2.

Similar experiments have been carried out on the effect of added water with other ceria-containing mixed oxides downstream of Pt/SiO_2. The behaviour of CeO_2/SiO_2 (28) is very similar to that of BaO/SiO_2 in Fig. 10 while that of CeO_2–ZrO_2 closely resembled that of CeO_2/Al_2O_3 (Fig. 11), except that the time needed for HNCO to reach a steady-state concentration when first placed on stream

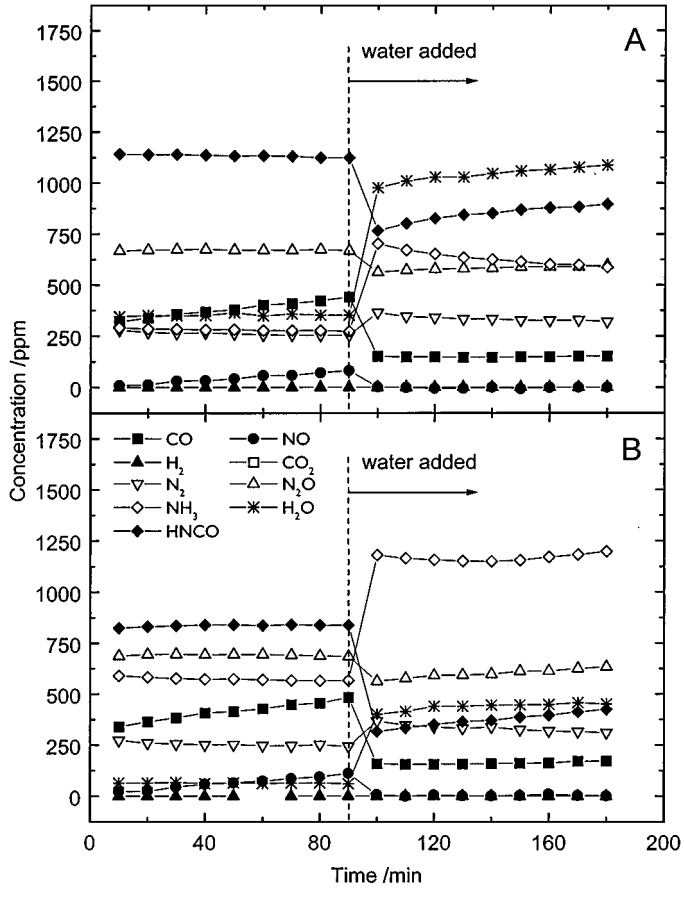

FIG. 10. Effect of adding ~1200 ppm water during the NO + CO + H_2 reaction at 315°C. (A) For 75 mg of Pt/SiO_2 alone. (B) With 75 mg of Pt/SiO_2 followed by 75 mg of SiO_2. Reactant concentrations and flowrates are the same as for Fig. 2.

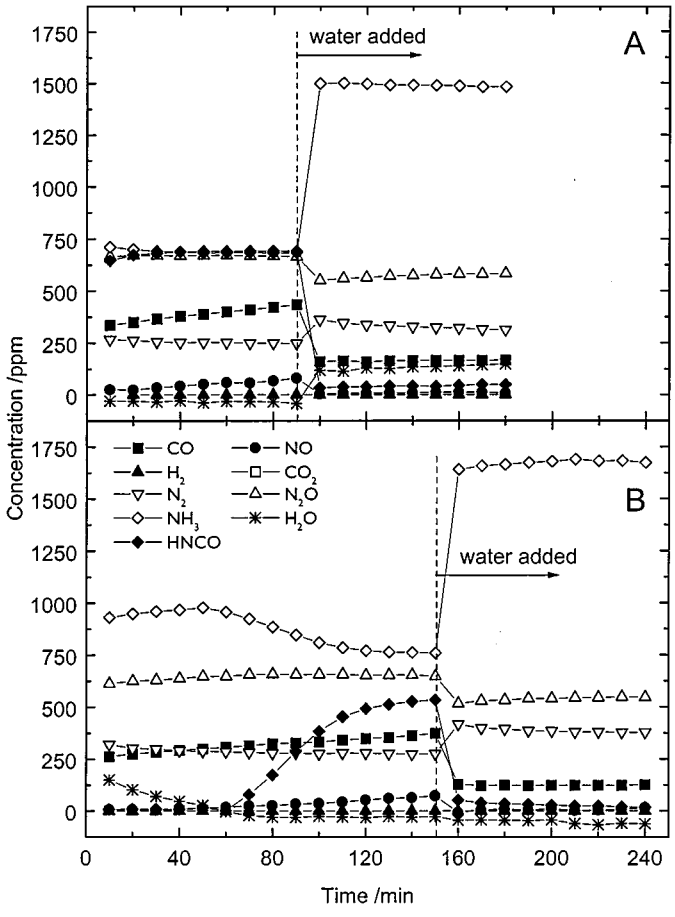

FIG. 11. Effect of adding ~1200 ppm water during the NO + CO + H_2 reaction at 315°C. (A) For 75 mg of Pt/SiO_2 followed by 75 mg of BaO/SiO_2. (B) For 75 mg of Pt/SiO_2 followed by 75 mg of CeO_2/Al_2O_3. Reactant concentrations and flowrates are the same as for Fig. 2.

with the dry feed was much shorter. CeO_2–ZrO_2 seemed especially active for hydrolysis since even a few fine particles remaining on the walls of a used reactor were sufficient to cause complete hydrolysis in subsequent tests with Pt/SiO_2 alone.

It is noticeable that conversions of both NO and CO increased after water was introduced for all four of the experiments illustrated in Figs. 10 and 11. This has nothing to do with the downstream oxides since it occurs to a similar degree with Pt/SiO_2 alone (Fig. 10A). As explained later, it appears to arise from a reaction of some of the additional NH_3, produced when H_2O is present, with NO and CO.

DISCUSSION

Reactions on the Metals

Table 1 compares the activity of the three metals in terms of the temperatures required to give a fixed turnover frequency of 0.02 molecules (NO) per surface atom per second (which corresponds to conversions of 13–37% with the standard concentrations). Comparison in terms of turnover frequencies at a fixed temperature is impractical because of the large extrapolations that would be needed to reach a common temperature. The activity order is Rh ≫ Pd ≫ Pt for the NO + CO reaction, but Pt ≫ Pd ≫ Rh for the NO + H_2 one. This is the same as for α-Al_2O_3-supported metals (40). The only difference for γ-Al_2O_3 is that Pd is slightly more active than Pt for the NO + H_2 reaction (19, 41). Although it has been suggested that the NO + H_2 reaction proceeds by hydrogen-assisted dissociation (42, 43), the most recent evaluation of single crystal data concludes that both reactions can be adequately explained by an initial direct dissociation of NO followed by removal of the fragments by adsorbed reductant (8), i.e.,

for the NO + H_2 reaction with S representing a surface site

$$NO_{ads} + S \rightarrow N_{ads} + O_{ads} \quad [5]$$

$$N_{ads} + NO_{ads} \rightarrow N_2O(g) + 2S \quad [6]$$

$$N_{ads} + N_{ads} \rightarrow N_2(g) + 2S \quad [7]$$

$$N_{ads} + 3H_{ads} \rightleftharpoons NH_{ads} + 2H_{ads} + S \rightleftharpoons NH_{2ads} + H_{ads} + 2S \rightarrow NH_3(g) + 4S \quad [8]$$

$$O_{ads} + 2H_{ads} \rightarrow H_2O(g) + 3S \quad [9]$$

and for NO + CO, reactions [5]–[7] plus

$$O_{ads} + CO_{ads} \rightarrow CO_2(g) + 2S. \quad [10]$$

The activity pattern for the two reactions can be interpreted in terms of these steps as follows. On rhodium, NO adsorbs in preference to CO and readily dissociates with creation of a surface that, depending on temperature, may contain both adsorbed NO and nitrogen atoms under reaction conditions (5). The rate is limited by the availability of sites for NO dissociation and nitrous oxide is the favoured product. As long as any NO remains, these processes are little affected by the reductant. Thus the two binary reactions can be expected to exhibit rather similar rates (and selectivities to N_2O) on rhodium as observed here (Table 1).

TABLE 1

Comparison of Activities for Reactions over Pt/SiO_2, Pd/SiO_2, and Rh/SiO_2[a]

Reaction	Pt/SiO_2	Pd/SiO_2	Rh/SiO_2
NO + H_2	60°C	96°C	202°C
NO + CO	285°C	261°C	213°C
NO + CO + H_2	183°C	127°C	196°C

[a] Temperatures giving a turnover frequency of 0.02 molecules(NO)/surface atom/second with standard conditions of CO = 3400 ppm, H_2 = 1000 ppm, and with NO = 2000 ppm for the NO + H_2 reaction, but 2800 ppm for the NO + CO and NO + CO + H_2 reactions.

On platinum, NO is adsorbed less strongly and displaced by CO (44). Hence the NO + CO reaction is strongly inhibited by CO and slower than on rhodium. The NO + H_2 reaction is free of this inhibition. Dissociation of NO is possible at room temperature on some crystal planes of platinum (8), and formation of N_2O by the N + NO step is possible at temperatures as low as 100 K (45). This allows the NO + H_2 to be much faster on Pt than Rh. Palladium is closer to Pt in respect of CO adsorption, which is inhibiting for the NO + CO reaction (46), but like Rh, the coverage by nitrogen atoms may be significant (47), and hence it exhibits intermediate behaviour.

It should be noted that the above considerations for rhodium apply strictly only when NO is in stoichiometric excess and no ammonia is formed, as is the case for the data in Fig. 6A. With hydrogen in excess the rate of the NO + H_2 reaction becomes faster than the NO + CO one (42) with considerable formation of ammonia, as found here when using a 2 : 5 NO/H_2 ratio. With a 2 : 1 mixture, formation of ammonia was confined to Pt/SiO_2 and Pd/SiO_2 at temperatures above those giving complete hydrogen conversion (Figs. 1A and 3A) and may be a consequence of mass transfer restrictions (i.e., the initial step, [5], occurs rapidly in a narrow section at the front of the bed where diffusion of NO to the metal surface is insufficient to maintain high NO coverage). This would allow build-up of nitrogen adatoms which can then be hydrogenated to NH_3 using hydrogen adatoms made available through the higher diffusion rate of H_2 compared with NO. The fall-off in NH_3 production above 200°C in these systems may be a partial consequence of secondary reactions in the rear of the bed, for example,

$$6NO + 4NH_3 \rightarrow 5N_2 + 6H_2O, \qquad [11]$$

which is relatively fast on platinum at these temperatures (48).

Reactions of the Ternary H_2 + NO + CO Mixture

The ternary reactions exhibit a number of unique features not predictable from the behaviour of the binary reactions. Most notable is the formation of HNCO in each system. The most probable route is via the combination of adsorbed hydrogen atoms with small numbers of isocyanate species which exist on the metals in equilibrium with N atoms and adsorbed CO, that is,

$$N_{ads} + CO_{ads} \rightleftharpoons NCO_{ads} + S \qquad [12]$$

$$NCO_{ads} + H_{ads} \rightarrow HNCO(g) + 2S. \qquad [13]$$

Metal-bound isocyanate groups are known for all three PGMs from infrared studies (16). They can be observed during the NO + CO reaction on Rh (15, 49), but not with Pt or Pd. Nonetheless, their existence in small numbers can be inferred from the rapid production of more stable support-bound NCO groups under reaction conditions (50, 51). These form either by direct spillover or perhaps by the short-range transport of HNCO generated using the hydrogen in neighbouring hydroxyl groups (52). In the ternary reaction system, adsorbed hydrogen and nitrogen atoms are continuously created, and this provides the driving force for the generation of HNCO as a gaseous product.

The amount of HNCO formed is much higher with Pt/SiO_2 than either Pd/SiO_2 or Rh/SiO_2. This is consistent with the especially strong adsorption of CO on Pt which maximises the concentration of CO in proximity to N atoms, thus favouring formation of metal-bound NCO and then HNCO. However, consideration of product distributions at different temperatures reveals a number of complexities in the Pt/SiO_2 system. For example, at 236°C when the conversion of H_2 is already complete, the amount of CO_2 produced by the NO + CO + H_2 reaction is much greater than that for the NO + CO reaction (Table 2). Likewise the amount of NH_3 made is much greater than that observed for the NO + H_2 reaction and is similar in concentration to that of CO_2. It seems probable that, despite the relatively low temperature, they are both arising from the same source: the hydrolysis of HNCO. The overall product distribution is best described as the sum of

$$NO + CO + 1.5H_2 \rightarrow HNCO + H_2O \qquad [14]$$

and

$$HNCO + H_2O \rightarrow NH_3 + CO_2, \qquad [4]$$

with a smaller contribution from the NO + H_2 reaction

$$2NO + H_2 \rightarrow N_2O + H_2O. \qquad [3]$$

This agrees with previous conclusions (27).

Above 260°C, formation of CO_2 increases steeply while that of NH_3 (and also H_2O) declines (Fig. 2). It is in this region that HNCO production grows most strongly to a maximum at 315°C which is close to a minimum in NH_3 formation. It seems highly unlikely that the extra HNCO arises directly from input H_2, which must be completely consumed towards the front of the bed. Likewise it cannot be attributed to H_2 arising from the water–gas shift

TABLE 2

Product Distributions for the Binary and Ternary Reactions over Pt/SiO_2 at 236°C[a]

Reaction	Product concentrations (ppm)					
	N_2O	N_2	NH_3	H_2O	CO_2	HNCO
NO + H_2	293	417	5	1145	—	—
NO + CO	~24	~4	—	—	~74	—
NO + CO + H_2	115	30	434	544	382	317

[a] Data for the NO + CO + H_2 reaction taken from Fig. 2, with the NO + H_2 and NO + CO reactions by interpolation between data points on Figs. 1A and 1B, respectively.

TABLE 3

Formation of HNCO by Reaction of NO and CO with NH_3 Compared with H_2[a]

Catalyst	Temperature °C	Input concentrations, ppm NO	CO	H_2	NH_3	HNCO, ppm
Pt/SiO_2	315	2800	3100	1160	none	1100
		2800	3100	none	1140	1200
		2800	3100	none	245	650
Pd/SiO_2	296	2900	3300	1180	none	600
		2900	3300	none	1170	800
Pd/SiO_2	282	1000	2400	none	400	300

[a] Using 75 mg of catalyst with total flowrate of 100 cm^3/min.

reaction since estimates based on the data of Grenoble *et al.* (53) for a Pt/SiO_2 catalyst with similar dispersion indicate that the rate of formation will be orders of magnitude too slow under the present conditions. The clear implication is that much of the HNCO must be formed by reuse of NH_3 formed towards the front of the bed through reactions [14] and [4].

Table 3 shows the results of several tests of this hypothesis. With both Pt/SiO_2 and Pd/SiO_2, ~1150 ppm of ammonia is slightly more efficient in forming HNCO than a equivalent concentration of hydrogen. With a lower NH_3 concentration of 245 ppm, Pt/SiO_2 generates 650 ppm HNCO, a remarkably high hydrogen selectivity of ~88%. Since thermodynamics do not allow the formation of significant amounts of HNCO from NH_3 and CO alone, the process must be driven by the dissociation of endogonic NO. The most efficient stoichiometry is

$$NH_3 + 2NO + 5CO \rightarrow 3HNCO + 2CO_2. \qquad [15]$$

As one would then anticipate, and seen in Fig. 2, HNCO formation peters out in the NO + CO + H_2 system once all NO is consumed at ~315°C. At higher temperatures still, HNCO hydrolysis dominates and NH_3 concentrations grow since recycling back to HNCO becomes impossible. It may be noted that reaction [15], coming on top of reactions [14] and [4], represents an amplification in the HNCO concentration by a factor of 3, which does approximate the increase in HNCO yield between the shoulder in its formation at 250°C and the maximum yield at 315°C.

The characteristics of the NO + CO + H_2 reaction on Pd/SiO_2 are rather different from those for Pt/SiO_2. The reaction of H_2 is much less inhibited by CO (Table 1), and from 100 to 230°C the NO + H_2 proceeds largely in parallel with the slower NO + CO reaction (Fig. 4) as noted earlier. Formation of HNCO, commencing at 235°C, is accompanied by a reduction in the amount of NH_3. As with the second stage of HNCO formation over Pt/SiO_2, this is best explained in terms of a reaction between NO, CO, and NH_3, Eq. [15], but in this case using the small amounts of NH_3 arising directly from the NO + H_2 reaction at the front of the catalyst bed. Data for Pd/SiO_2 in Table 3 show that this is feasible. Again HNCO concentrations start to decline at the point where NO consumption is complete.

The behaviour of Rh/SiO_2 for the NO + CO + H_2 reaction (Fig. 6) exhibits a third pattern. The maximum yield of HNCO is even less than with Pd/SiO_2 and confined to a narrow interval near 225°C. Formation of NH_3 increases above that temperature to a maximum of 700 ppm near 260°C despite the fact that ammonia is not a product of the NO + H_2 reaction with the standard 2 : 1 mixture (Fig. 7). Most significantly, the peak in HNCO concentration coincides with total NO consumption while the increase in NH_3 is matched by a drop in water formation. The implication is that HNCO is still being made, by reaction [14], at temperatures above its maximum yield, but is being hydrolysed to NH_3, reaction [4], which cannot be recycled to HNCO for lack of NO. Thus the primary reason for the low yield of HNCO with Rh/SiO_2 under the conditions used here is that total consumption of H_2 and NO is near coincident (because NO is simultaneously consumed by reaction with CO). With Pt/SiO_2 and Pd/SiO_2, the NO + CO reaction is much slower than the NO + H_2 one which provides a wide gap in temperature between the total consumption of H_2 and that of NO, a gap in which NO, CO, and NH_3 may coexist and generate HNCO via the secondary reaction, Eq. [15].

The above considerations suggest that HNCO formation will be very dependent on reaction conditions. Hecker and Bell (31), using a reduced 4.6% Rh/SiO_2 catalyst and 4- to 20-fold higher pressures than here, observed ammonia (in 19% yield) at 180°C plus a solid product, identified as urea $(NH_2)_2CO$, in 12% yield. They concluded from mass balance calculations that the corresponding preoxidised catalyst gave a different solid product, with a C/N ratio of 1.0, in a 42% yield which they suspected, but were unable to prove, was HNCO. The present results demonstrate that gaseous HNCO can indeed be formed. In our experience conversion of HNCO to solid products, by polymerisation or reaction with ammonia, is difficult to avoid unless the entire analysis system is heated, with a temperature of 90°C being satisfactory for the concentrations produced here. The urea observed by Hecker and Bell (31) probably arose through combination of HNCO with ammonia, being produced in excess, in cooler sections of their system.

According to Voorhoeve and Trimble (21), urea will be formed if the condensation is carried out at an elevated temperature, but ammonium cyanate (NH_4OCN) is formed instead at room temperature. The products they report for unsupported PGMs, HNCO with Pd but NH_4OCN with Pt and Rh (21–24) conform to the tendency to form ammonia observed here (i.e., least with Pd/SiO_2). However, they observed much higher yields: 60% HNCO with Pd and >90% NH_4OCN (i.e., 45% isocyanate) for Pt and Rh. The lower

yields here can be partly attributed to the effect of hydrolysis on the metal/support combination. While reaction with NO and CO does allow some reconversion of ammonia produced by hydrolysis of HNCO, reaction [15], it necessarily requires dissociation of NO which increases the scope for diversion of nitrogen atoms to other products. Voorhoeve and Trimble also used higher temperatures which, coupled with much higher CO pressures (50,000 ppm vs 3400 ppm here), is sure to aid in the capture of N atoms as metal-bound NCO groups and then HNCO.

HNCO Hydrolysis on Oxides

It is apparent from Fig. 10 that SiO_2 alone has some modest activity for the hydrolysis of HNCO. The amount of HNCO produced from NO + CO + H_2 over Pt/SiO_2 is reduced when SiO_2 is placed downstream and, with or without this SiO_2 present, it falls further when water is added. However, the conversion to NH_3 and CO_2 is only partial even at 315°C. The implication of the above discussion concerning ammonia formation is that the PGM/silica catalysts are more active than SiO_2 alone for hydrolysis. This appears especially so for Rh/SiO_2 where the generation of NH_3 from NO + CO + H_2, but not from NO + H_2, at temperatures above 230°C can be explained in terms of HNCO hydrolysis. Higher hydrolysis activity is not unreasonable since HNCO formed at the front of the bed may undergo dissociation on metal particles downstream, a known process on PGMs (14), thus facilitating contact between isocyanate groups and adjacent water molecules or surface hydroxyl groups in a process which is additional to that on silica alone. Water may undergo dissociation on the metal, thus facilitating hydrolysis of support-bound isocyanates which is also much faster on Pt/SiO_2 than on SiO_2 (52).

It is clear that other oxide supports are much more active than silica for HNCO hydrolysis. As shown by Figs. 9 and 11, CeO_2–ZrO_2, CeO_2/Al_2O_3, and BaO/SiO_2 give complete reaction to the limit of the water available. The same is true for CeO_2/SiO_2 (28) and for Al_2O_3 alone (27). Hydrolysis of isocyanic acid may be either acid- or base-catalysed (54) and the ease with which it occurs on the range of oxides tested here indicates that weak sites of either type will suffice.

Several recent studies (55–57) have shown that modern vehicles emit significant quantities of ammonia with concentrations up to 1,400 ppm being found in one study (57). Formation of ammonia is of environmental importance since it contributes to the formation of atmospheric haze through combination with NO_x and SO_x to make ammonium salts (56). The present results indicate that the generation of isocyanic acid as an intermediate is a probable contributor to ammonia formation with three-way catalysts. It is incorrect to assume that HNCO cannot form when oxygen is present. Previous work shows that isocyanic acid formation continues as long as the amount of oxygen does not exceed that required for removal of all carbon monoxide (29). Ammonia, probably derived from isocyanic acid, is also seen during light-off with complex mixtures, that are marginally lean overall, on alumina-supported PGMs (30). The pattern of ammonia formation for the individual metals resembles that for HNCO here. However, HNCO formation does require significant CO coverages, which means that it cannot form when CO is fully consumed with oxygen in excess or at temperatures where equilibrium CO coverages are low. This probably confines the isocyanic acid-to-ammonia route to <400°C on vehicles. In any event, isocyanic acid itself is highly unlikely to exist in exhaust under any circumstances since the high water content will inevitably ensure complete hydrolysis on the active oxide washcoats used in catalytic converters.

CONCLUSIONS

The formation of HNCO is a characteristic feature of the NO + CO + H_2 reaction over silica-supported platinum, palladium, and rhodium. Under the conditions used here, Pt produces the largest amount, seemingly in two stages, firstly from H_2 and then using NH_3 being formed as a co-product. With Pd, HNCO arises largely from NH_3 alone because H_2 is totally removed by reaction with NO at low temperature. Rhodium gives rise to the least HNCO. Formation is confined to a narrow temperature region due to the coincident consumption of NO and H_2 which precludes reaction of NH_3 with NO and CO. Hydrolysis of HNCO to NH_3 and CO_2 is appreciable on SiO_2 alone and faster when a metal is present. Other oxide systems, both acidic and basic, give complete hydrolysis to the limit of the water present and total reaction with even small excesses of water. The possible presence of HNCO in vehicle exhaust is not an issue since the presence of a vast excess of steam and an active washcoat in three-way converters will ensure complete hydrolysis. However, the latter process may contribute to ammonia emissions at moderate temperatures under conditions where CO is still present.

ACKNOWLEDGMENTS

This work has been supported by grants from the Australian Research Council. The Pt/SiO_2 and Pd/SiO_2 catalysts used here were a past gift from Professor R. Burwell.

REFERENCES

1. Heck, R. M., and Farrauto, R. J., "Catalytic Air Pollution Control: Commercial Technology." Van Nostrand Reinhold, New York, 1995.
2. Peden, C. H. F., Belton, D. N., and Schmieg, S. J., *J. Catal.* **155**, 204 (1995).
3. Permana, H., Ng, K. Y. S., Peden, C. H. F., Schmieg, S. J., and Belton, D. N., *J. Phys. Chem.* **99**, 16344 (1995).
4. Permana, H., Ng, K. Y. S., Peden, C. H. F., Schmieg, S. J., Lambert, D. K., and Belton, D., *J. Catal.* **164**, 194 (1996).

5. Herman, G. S., Peden, C. H. F., Schmeig, S. J., and Belton, D. N., *Catal. Lett.* **62**, 131 (1999).
6. Cho, B. K., *J. Catal.* **138**, 255 (1992).
7. Cho, B. K., *J. Catal.* **148**, 697 (1994).
8. Nieuwenhuys, B. E., *Adv. Catal.* **44**, 259 (2000).
9. Unland, M. L., *Science* **179**, 567 (1973).
10. Unland, M. L., *J. Catal.* **31**, 459 (1973).
11. Unland, M. L., *J. Phys. Chem.* **77**, 1952 (1973).
12. Dalla Betta, R. A., and Shelef, M., *J. Mol. Catal.* **1**, 431 (1975).
13. Solymosi, F., Völgyesi, L., and Raskó, J., *Z. Phys. Chem.* **120**, 79 (1980).
14. Solymosi, F., and Bánsági, T., *J. Phys. Chem.* **83**, 552 (1979).
15. Hecker, W. C., and Bell, A. T., *J. Catal.* **85**, 389 (1984).
16. Solymosi, F., and Raskó, J., *Appl. Catal.* **10**, 19 (1984).
17. Kiss, J., and Solymosi, F., *J. Catal.* **179**, 277 (1998).
18. Matyshak, V. A., and Krylov, O. V., *Catal. Today* **25**, 1 (1995).
19. Kobylinski, T. P., and Taylor, B. W., *J. Catal.* **33**, 376 (1974).
20. Shelef, M., and Gandhi, H. S., *Ind. Eng. Chem. Prod. Res. Dev.* **11**, 393 (1972).
21. Voorhoeve, R. J. H., Trimble, L. E., and Freed, D. J., *Science* **200**, 759 (1978).
22. Voorhoeve, R. J. H., and Trimble, L. E., *J. Catal.* **53**, 251 (1978).
23. Voorhoeve, R. J. H., and Trimble, L. E., *Science* **202**, 525 (1978).
24. Voorhoeve, R. J. H., and Trimble, L. E., *J. Catal.* **54**, 269 (1978).
25. Voorhoeve, R. J. H., and Trimble, L. E., *in* "Chemical Industries: Catalysis of Organic Reactions," Vol. 5, p. 289. Dekker, New York, 1981.
26. Dümpelmann, R., Cant, N. W., and Trimm, D. L., *Appl. Catal. B* **6**, L291 (1995).
27. Dümpelmann, R., Cant, N. W., and Trimm, D. L., *J. Catal.* **162**, 96 (1996).
28. Cant, N. W., Chambers, D. C., Cowan, A. D., Liu, I. O. Y., and Satsuma, A., *Top. Catal.* **10**, 13 (2000).
29. Dümpelmann, R., Cant, N. W., and Cowan, A. D., *Stud. Surf. Sci. Catal.* **101**, 1175 (1996).
30. Cant, N. W., Angove, D. E., and Chambers, D. C., *Appl. Catal. B* **17**, 63 (1998).
31. Hecker, W. C., and Bell, A. T., *J. Catal.* **88**, 289 (1984).
32. Takahashi, N., Shinjoh, H., Iijima, T., Suzuki, T., Yamazaki, K., Yokota, K., Suzuki, H., Miyoshi, N., Matsumoto, S.-I., Tanizawa, T., Tanaka, T., Tateshi, S.-S., and Kasahara, K., *Catal. Today* **27**, 63 (1996).
33. Griffith, D. W. T., *Appl. Spectrosc.* **50**, 59 (1996).
34. Rothman, L., Gamache, R., Tipping, R., Rinsland, C., Smith, M., Benner, D., Malathy Devi, V., Flaud, J. M., Camy-Peyret, C., Perrin, A., Goldman, A., Massie, S., Brown, L., and Toth, R., *J. Quant. Spectrosc. Radiat. Transfer* **48**, 469 (1992).
35. Uchijima, T., Herrman, J. M., Inoue, Y., Burwell, R. L., Butt, J. B., and Cohen, J. B., *J. Catal.* **50**, 464 (1977).
36. Pitchai, R., Wong, S. S., Takahashi, N., Butt, J. B., Burwell, R. L., and Cohen, J. B., *J. Catal.* **94**, 478 (1985).
37. Bauerle, G. L., and Nobe, K., *Ind. Eng. Chem. Prod. Res. Dev.* **13**, 185 (1974).
38. Mergler, Y. J., and Nieuwenhuys, B. E., *Appl. Catal. B* **12**, 95 (1997).
39. Dümpelmann, R., Cant, N. W., and Trimm, D. L., *Catal. Lett.* **32**, 357 (1995).
40. Shinjoh, H., Muraki, H., and Fujitani, Y., *Stud. Surf. Sci. Catal.* **30**, 187 (1987).
41. Taylor, K. C., and Klimisch, R. L., *J. Catal.* **30**, 478 (1973).
42. Hecker, W. C., and Bell, A. T., *J. Catal.* **92**, 247 (1985).
43. Burch, R., and Watling, T. C., *Catal. Lett.* **37**, 51 (1996).
44. Brown, M. F., and Gonzalez, R. D., *J. Catal.* **44**, 477 (1976).
45. Wang, H., Tobin, R. G., DiMaggio, C. L., Fisher, G. B., and Lambert, D. K., *J. Chem. Phys.* **107**, 9569 (1997).
46. Holles, J. H., Switzer, M. A., and Davis, R. J., *J. Catal.* **190**, 247 (2000).
47. Rainer, D. R., Vesecky, S. M., Koranne, M., Oh, W. S., and Goodman, D. W., *J. Catal.* **167**, 234 (1997).
48. Otto, K., Shelef, M., and Kummer, J. T., *J. Phys. Chem.* **74**, 2690 (1970).
49. Chafik, T., Kondarides, D. I., and Verykios, X. E., *J. Catal.* **193**, 303 (2000).
50. Chang, C. C., and Hegedus, L. L., *J. Catal.* **57**, 361 (1979).
51. Almusaiteer, K., and Chuang, S. S. C., *J. Catal.* **184**, 189 (2000).
52. Lorimer, D'A., and Bell, A. T., *J. Catal.* **59**, 223 (1979).
53. Grenoble, D. C., Estadt, M. M., and Ollis, D. F., *J. Catal.* **67**, 90 (1981).
54. March, J., "Advanced Organic Chemistry," p. 786. Wiley, New York, 1985.
55. Laurikko, J., *Int. J. Vehicle Des.* **20**, 159 (1998).
56. Fraser, M. P., and Cass, G. R., *Environ. Sci. Technol.* **32**, 1053 (1998).
57. Baum, M. M., Kiyomiya, E. S., Kumar, S., and Lappas, A. M., *Environ. Sci. Technol.* **34**, 2851 (2000).